Since January 2020 Elsevier has created a COVID-19 resource centre with free information in English and Mandarin on the novel coronavirus COVID-19. The COVID-19 resource centre is hosted on Elsevier Connect, the company's public news and information website.

Science of the Total Environment 745 (2020) 141023

Contents lists available at ScienceDirect

Science of the Total Environment

journal homepage: www.elsevier.com/locate/scitotenv

Non-negligible impacts of clean air regulations on the reduction of tropospheric NO_2 over East China during the COVID-19 pandemic observed by OMI and TROPOMI

Guanyu Huang [a,*], Kang Sun [b,c]

[a] Environmental and Health Sciences Program, Spelman College, 350 Spelman LN SW, Atlanta, GA 30314, USA
[b] Department of Civil, Structural and Environmental Engineering, University at Buffalo, 212 Ketter Hall, Buffalo, NY 14228, USA
[c] Research and Education in eNergy, Environment and Water (RENEW) Institute, University at Buffalo, 112 Cooke Hall, Buffalo, NY 14228, USA

HIGHLIGHTS

- Tropospheric NO_2 decreased sharply over East China in 2020 lunar new year holiday.
- These reductions of tropospheric NO_2 were driven by COVID-19 lockdowns and clean air regulations.
- Relative contributions of COVID-19 lockdowns and clean air regulations varied by region.

GRAPHICAL ABSTRACT

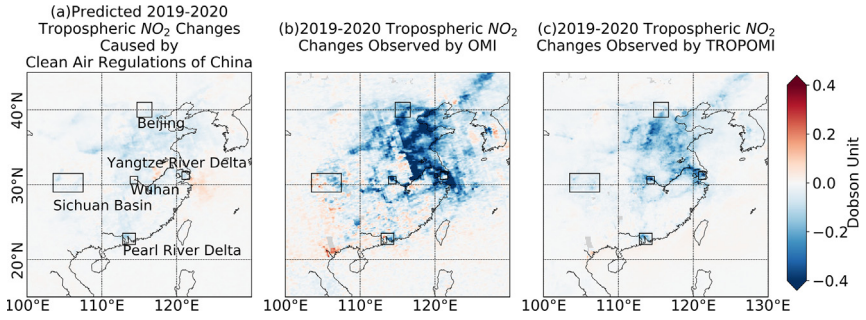

ARTICLE INFO

Article history:
Received 18 June 2020
Received in revised form 10 July 2020
Accepted 15 July 2020
Available online 21 July 2020

Keywords:
COVID-19
Tropospheric NO_2
OMI
TROPOMI
Air quality

ABSTRACT

We study the variation of tropospheric NO_2 vertical column densities (TropNO_2VCDs) over East China during the 2005–2020 lunar new year (LNY) holiday seasons to understand factors on the reduction of tropospheric NO_2 during the outbreak of COVID-19 in East China using Ozone Monitoring Instrument (OMI) and TROPOspheric Monitoring Instrument (TROPOMI) observations. TropNO_2VCDs from OMI and TROPOMI reveal sharp reductions of 33%–72% during 2020 LNY holiday season and the co-occurring outbreak of COVID-19 relative to the climatological mean of 2005–2019 LNY holiday seasons, and 22%–67% reduction relative to the 2019 LNY holiday season. These reductions of TropNO_2VCD occur majorly over highly polluted metropolitan areas with condensed industrial and transportation emission sources. COVID-19 control measures including lockdowns and shelter-in-place regulations are the primary reason for these tropospheric NO_2 reductions over most areas of East China in 2020 LNY holiday season relative to the 2019 LNY holiday season, as COVID-19 control measures may explain ~87%–90% of tropospheric NO_2 reduction in Wuhan as well as ~62%–89% in Beijing, Yangtze River Delta (YRD) and Sichuan Basin areas. The clean air regulation of China also contributes significantly to reductions of tropospheric NO_2 simultaneously and is the primary factor in the Pearl River Delta (PRD) area, by explaining ~56%–63% of the tropospheric NO_2 reduction there.

1. Introduction

The COVID-19 disease caused by SARS-CoV-2, a novel coronavirus, was first reported in Wuhan, capital of Hubei Province in China, in December 2019 (Li et al., 2020). This disease had spread quickly in

* Corresponding author.
E-mail addresses: ghuang@spelman.edu (G. Huang), kangsun@buffalo.edu (K. Sun).

https://doi.org/10.1016/j.scitotenv.2020.141023
0048-9697/

Wuhan city and surrounding areas with 258 confirmed cases on January 21, 2020 (World Health Organization, 2020). By then, confirmed cases were also found in Japan, South Korea, Thailand and eventually worldwide, respectively (World Health Organization, 2020). The Chinese government had announced a strict lockdown and shelter-in-place law in Wuhan City on January 23, 2020 (Li et al., 2020; Tian et al., 2020). These regulations required people to stay at home without using cars, suspended all public transportations and closed non-essential businesses and manufacturing factories. A day later, other cities in Hubei province also conducted similar lockdown and shelter-in-place regulations (Tian et al., 2020). In the following week, the government of China had announced mandatory "shelter-in-place" orders nationwide. These COVID-19 control measures and consequently minimized human activities in China and worldwide are expected to result in substantially reduced NO_x ($NO_x = NO+NO_2$) emissions due to the dominancy of anthropogenic NO_x sources (Bauwens et al., 2020; Collivignarelli et al., 2020; Earth Observatory NASA, 2020; Lian et al., 2020; Liu et al., 2020).

Meanwhile, the outbreak of COVID-19 happened during the 2020 lunar new year (LNY) holiday season (a.k.a. spring festival) as the 2020 LNY's day was January 25, 2020 based on the lunar calendar. The LNY holiday season in China usually lasts for approximately 40 days and is herein defined as 14 days before the LNY's day and 25 days after (Fig. 1). During the LNY holiday season, the tropospheric NO_2 abundance over China indicates "holiday effects" that are characterized by two high peaks before/after the national LNY holiday and a trough in the middle. This pattern shifts with the LNY's day on the Julian calendar (Tan et al., 2009; Zhang et al., 2019; more in Section 2.1). The COVID-19 lockdown in China started on January 23, 2020 and lasted through the entire 2020 LNY holiday season. As a result, studies on tropospheric NO_2 variation during the outbreak of COVID-19 shall take account of the impacts of LNY holiday seasons and shifts of LNY days on the Julian calendar every year (Liu et al., 2020).

Also, China has begun to conduct new emission regulations since 2010, after which tropospheric NO_2 has been decreasing rapidly nationwide (de Foy et al., 2016; Lin et al., 2019; Liu et al., 2016). These clean air regulations may also contribute to the observed tropospheric NO_2 reduction during the outbreak of COVID-19 in China.

Significant reduction in tropospheric NO_2 vertical column densities ($TropNO_2VCDs$) was observed by satellite instruments during the COVID-19 lockdown period (Bauwens et al., 2020; Liu et al., 2020), which may be caused by a combination of "holiday effects" of LNY, meteorological conditions, control measures and lockdowns due to the COVID-19 outbreak, and the continuation of clean air regulations in China. The LNY "holiday effects" of $TropNO_2VCDs$ can be canceled out since this study only focuses $TropNO_2VCDs$ over LNY holiday seasons. The meteorological influences on tropospheric NO_2 should be small in this study because meteorological conditions were normal in 2020 LNY holiday seasons compared to the 2005–2019 climatology, and 40-day average $TropNO_2VCDs$ smooth out most weather induced variability (European Centre for Medium-Range Weather Forecasts, 2020; more discussions in Section 4.2).

As such, the goal of this study is to understand the variation of $TropNO_2VCDs$ in East China during the 2005–2020 LNY holiday seasons and quantify contributions by both COVID-19 control measures and clean air regulations to the reduction of $TropNO_2VCDs$ during 2020 LNY holiday season in East China. We combine tropospheric NO_2 observations from Ozone Monitoring Instrument (OMI) with moderate spatial resolutions and long-term coverage and TROPspheric Monitoring Instrument (TROPOMI) with fine resolutions but only available in 2019–2020 LNY holiday seasons.

2. Materials and data

2.1. Lunar new year holiday season

The LNY day is set according to the lunar calendar and varies from late January to early February on Julian calendars. Fig. 1 shows the distribution of LNY days and the official national holidays during 2005–2020. Millions of people in mainland China return to their hometowns from working places in the beginning of the holiday season and travel back to work sites towards the end of the holiday season (Li et al., 2016). The LNY holiday season with a large migration usually lasts approximately 40 days, 14 days before the LNY's day and 25 days after, as shown in Fig. 1. The industrial and transportation-related emissions decrease before the LNY's day, stay at a relatively low level during the LNY holiday, and then gradually increase back to normal after the holiday. The consequent impact on air pollution levels is known as the "holiday effect" that shifts with LNY days (Feng et al., 2016; Huang et al., 2012; Ji et al., 2018; Tan et al., 2009; Yao et al., 2019). As shown in Fig. 1, the variation of LNY dates on the Julian calendar is blurred since we averaged over a 40-day period. The natural emissions of NO_x are considerably small during LNY periods (January to early March)

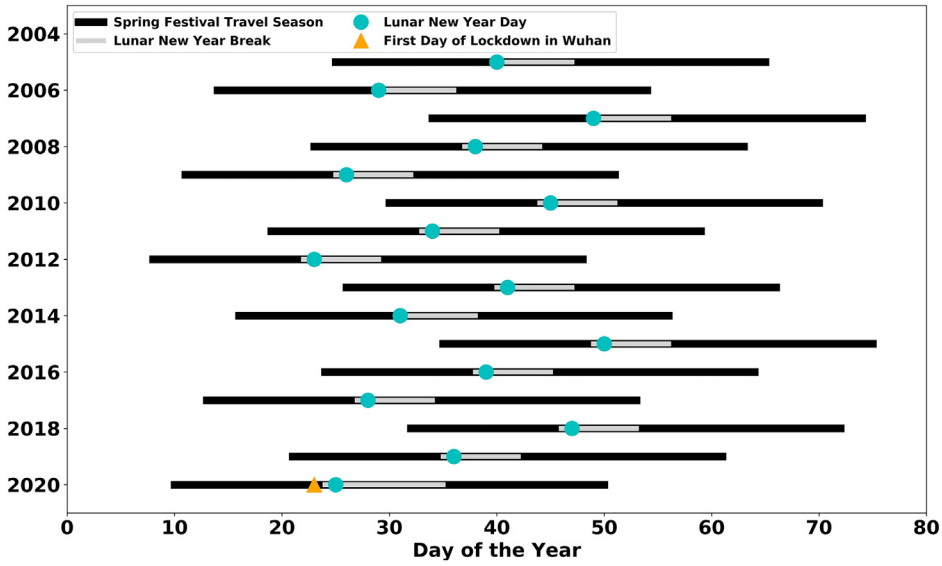

Fig. 1. Lunar new year (LNY) day and national holidays in 2005–2020 are marked by cyan dots and solid gray lines, respectively. Solid black lines represent LNY holiday seasons during 2005–2020. The first day of lockdown in Wuhan is marked by the orange triangle for 2020. Note that LNY national holidays in 2020 had been extended from 7 days to 10 days due to the COVID-19.

because of low temperature, low level of lighting and inactive biosphere (Lin, 2012). The dominant contributor to NO_2 variation is anthropogenic emission that shifts with the lunar calendar. As a result, studies on tropospheric NO_2 variation during the outbreak of COVID-19 shall take account of the impacts of LNY holiday seasons and shifts of LNY days on the Julian calendar every year.

2.2. OMI and TROPOMI observations

Level 2 OMI tropospheric NO_2 product (OMNO2 version SPv3) (Krotkov et al., 2019) and TROPOMI Tropospheric NO_2 product (version 1.3.0) (European Space Agency, 2018) are used in this study.

OMI is a push room UV-VIS spectrometer that measures the Earth's backscattered sunlight since October 2004 aboard the Aura satellite (Levelt et al., 2006). The Aura satellite is on a sun-synchronous polar orbit with an equator crossing time of approximately 1345 local time (Kroon et al., 2008; Levelt et al., 2006). The swath width of OMI is 2600 km, enabling global daily coverage with a resolution of 13 km × 24 km (along × across-track) at nadir. The OMI level 2 NO_2 standard product is retrieved through a variation of differential optical absorption spectroscopy algorithm (Bucsela et al., 2013; Krotkov et al., 2017). OMI has been proved with considerably stable performance since the launch in 2004, although OMI's global coverage and data sampling have been affected by the "row anomaly" that was first found in 2007 (Krotkov et al., 2017). The impacts of row anomaly on data sampling are shown in Fig. S1. As a result, only OMI tropospheric NO_2 observations of rows 5–23 on clear sky scenes (with cloud coverage less than 0.3) are used, excluding those affected by the row anomaly, to avoid inconsistent sampling of data (Duncan et al., 2016; Krotkov et al., 2017; Krotkov et al., 2019).

TROPOMI is the single payload aboard the Sentinel 5 Precursor (S5P) satellite that has a sun-synchronous orbit with local overpass time of approximately 1330 with a near-daily global coverage since April 2018 (Veefkind et al., 2012). The TROPOMI NO_2 retrieval algorithm is developed by the Royal Netherlands Meteorological Institute and based on the NO_2 DOMINO (Dutch OMI NO2) algorithm with significant improvements. TROPOMI measures tropospheric NO_2 with a pixel size of 7 km × 3.5 km at nadir, and the resolution has been improved to 5.5 km × 3.5 km with a change in the S5P operation scenario since August 6, 2019 (orbit 9388) (Eskes and Eichmann, 2019). Similar to OMI data, we only use TROPOMI observations with cloud coverage less than 0.3 (Eskes and Eichmann, 2019). Although TROPOMI recommended pixels with quality assurance (QA) values greater than 0.75, we use TROPOMI pixels with QA values greater than 0.5, which includes good quality retrievals over clouds and over snow/ice scenes and is "useful for assimilation and model and model comparison studies" (Eskes and Eichmann, 2019), to add more observations to this study in wintertime. In addition, since pixels with QA greater than 0.75 removes cloud scenes with cloud coverage greater than 0.5 (Eskes and Eichmann, 2019), we use a stricter threshold (<0.3) for cloud coverage to remove pixels that may be influenced by clouds and maintain sampling consistency. Furthermore, the difference is small between selecting 0.5 and 0.75 for QA value thresholds with both cloud threshold (<0.3) applied in this study as shown in Fig. S2.

Consequently, the combination of OMI and TROPOMI provides us a long temporal coverage of TropNO2VCD observations with a moderate spatial resolution in 2005–2020 LNY holiday seasons and a fine spatial resolution in 2019–2020 LNY holiday seasons.

3. Methodology

3.1. Conversion of level 2 data to level 3 data

It is critical to ensure data consistency due to the use of long-term data from two spaceborne data sources. We produce level 3 data over

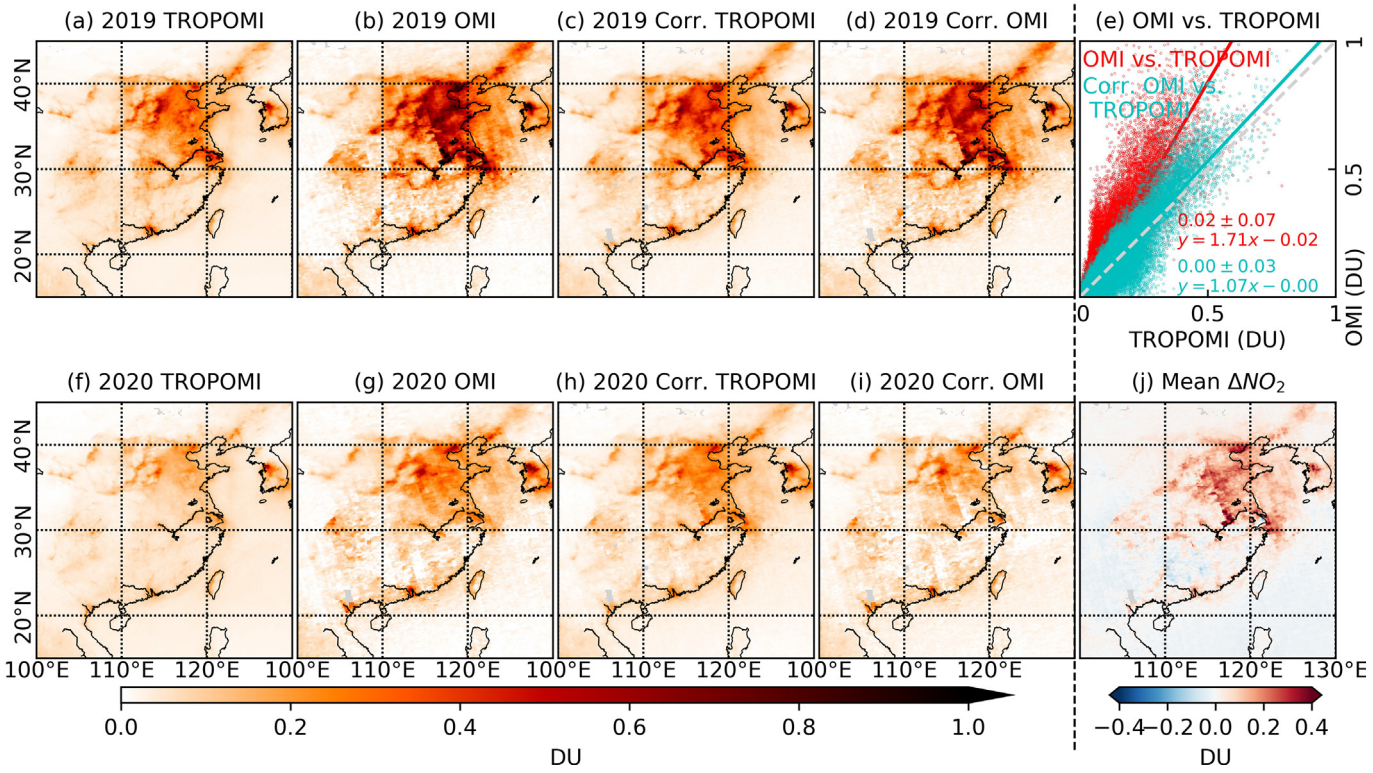

Fig. 2. Comparisons of OMI and TROPOMI observed tropospheric NO_2 vertical column densities (TropNO_2VCDs) during 2019 and 2020 lunar new year (LNY) holiday seasons. TropNO_2VCDs observed by OMI and TROPOMI during 2019 and 2020 LNY holiday seasons are shown in panels (a), (b), (f) and (g), respectively. OMI and TROPOMI with corrections applied are shown in panels of (c), (d), (h) and (i), respectively. Scatter plots of TROOMI tropospheric NO_2 vs. OMI NO_2 and corrected TROPOMI vs. corrected OMI tropospheric NO_2 during 2019 and 2020 LNY holiday season in panel (e). Panel (j) shows a map of the mean difference between OMI and TROPOMI TropNO_2VCDs averaged during 2019 and 2020 LNY holiday seasons (i.e., *c(i,j)* in Eq. 1).

LNY holiday seasons by averaging level 2 data to a common, regular 0.125° × 0.125° grid and apply corrections to these regridded level 3 tropospheric NO_2 data. We use the physical oversampling method by Sun et al. (2018) to average temporally and spatially level 2 satellite observations to level 3 grid. Two-dimensional super Gaussian functions are used to represent the spatial response functions of satellite sensors. In comparison with conventional approaches that only consider the pixel corners, this method gives considerable advantages of visualizing the distribution and local gradients of trace gases and for scenarios with short temporal windows (Sun et al., 2018). We directly regrid OMI level 2 data to the 0.125° × 0.125° grid, while we regrid TROPOMI level 2 data to 0.01° × 0.01° first and then aggregate them to 0.125° × 0.125° through area-weighted averaging (Sun et al., 2018; Zhu et al., 2017). This is because the physical oversampling method assumes that the sensitivity of a satellite observation is represented by a continuous spatial response function, which is feasible when the grid size is not significantly larger than the satellite footprint.

3.2. Corrections applied to OMI and TROPOMI level 3 data

The overpass times of OMI and TROPOMI are 1345 and 1330 local time, respectively (Levelt et al., 2006; Veefkind et al., 2012). It is reasonable to assume that OMI and TROPOMI have similar observations on tropospheric NO_2, since the lifetime of NO_2 in the troposphere is much longer than 15 min (Shah et al., 2020). OMI TropNO_2VCDs during 2019 and 2020 LNY holiday seasons (Fig. 2 (b) and (g)) are higher than TROPOMI TropNO_2VCDs (Fig. 2 (a) and (f)). Both years combined, OMI is higher than TROPOMI by 0.02 Dobson unit (DU) with 0.07 DU standard deviation as shown in panel (e) of Fig. 2. These biases are considerably higher over polluted areas, e.g., major metropolitan areas and the North China Plain. The regression slope between OMI and TROPOMI level 3 data is 1.71 (Fig. 2(e)). A similar difference between OMI and TROPOMI on tropospheric NO_2 was also found over China in January 2019 (Cheng et al., 2019). These discrepancies may be caused by many factors, including spectral fitting algorithms, atmospheric mass factor (AMF) calculation, and spatial sampling discrepancies due to different pixel size and OMI's row anomaly (OMI and TROPOMI spatial sampling on selected days in 2020 are shown in Fig. S3) (Cheng et al., 2019; Griffin et al., 2019; Krotkov et al., 2017). As a result, a correction should be applied to OMI and TROPOMI level 3 data to reconcile the discrepancies.

Since we focus on spatially regridded and temporally averaged TropNO_2VCDs over LNY holiday seasons in China instead of individual retrievals, we apply a simple correction to OMI and TROPOMI level 3 TropNO_2VCDs. We obtain mean differences between OMI and TROPOMI level 3 data during 2019 and 2020 LNY holiday seasons as:

$$c(i,j) = 0.5 \times [(OMI_{2019}(i,j) + OMI_{2020}(i,j)) - (TROPOMI_{2019}(i,j) + TROPOMI_{2020}(i,j))] \quad (1)$$

where *i, j* are latitude and longitude grid indices, respectively. OMI_{2019}, OMI_{2020}, $TROPOMI_{2019}$ and $TROPOMI_{2020}$ represent level 3 TropNO_2VCDs measured by OMI or TROPOMI during 2019 and 2020 LNY holiday seasons, respectively. The correction term *c(i,j)* accounts for the potential sampling and algorithm biases between the OMI and TROPOMI NO_2 products, which are assumed to be steady over all LNY holiday seasons. Therefore, we apply the same corrections to both OMI and TROPOMI level 3 data as follows: corrected OMI TropNO_2VCDs in LNY of year yi are defined as

$$corr.OMI_{yi}(i,j) = OMI_{yi}(i,j) - 0.5 \times c(i,j), \quad (2)$$

and corrected TROPOMI TropNO_2VCDs are defined as

$$corr.TROPOMI_{yi}(i,j) = TROPOMI_{yi} + 0.5 \times c(i,j), \quad (3)$$

A map of the correction term *c(i,j)* is shown in the panel (j) of Fig. 2. TropNO_2VCDs during 2019 and 2020 LNY holiday seasons after applying corrections are plotted in panels of (c), (d), (h) and (i) of Fig. 2, respectively. OMI TropNO_2VCDs after applying corrections shows significantly better agreement with TROPOMI observations with a mean bias of 0.00 +/− 0.03 DU as in panel (e) of Fig. 2.

4. Results

4.1. Distribution of tropospheric NO_2 during LNY holiday seasons in East China

Mean OMI TropNO_2VCDs during 2005–2019 LNY holiday seasons with corrections applied are plotted in panel (a) of Fig. 3. The panel (a) reveals large hotspots of TropNO_2VCDs over the North China plain and other metropolitan areas as labeled in the plot. High TropNO_2VCDs are seen over China. The mean TropNO_2VCDs are up to 0.47 DU and 0.68 DU in Pearl River Delta (PRD) and Yangtze River Delta (YRD) areas, respectively. The Beijing, Sichuan Basin and Wuhan areas show slightly lower TropNO_2VCDs as 0.25 DU, 0.16 DU and 0.37 DU, respectively.

Both OMI and TROPOMI with correction applied observed 0.1–0.4 DU reductions over East China in 2020 LNY holiday season relative to means of 2005–2019 LNY holiday seasons, as shown in panels (b) and

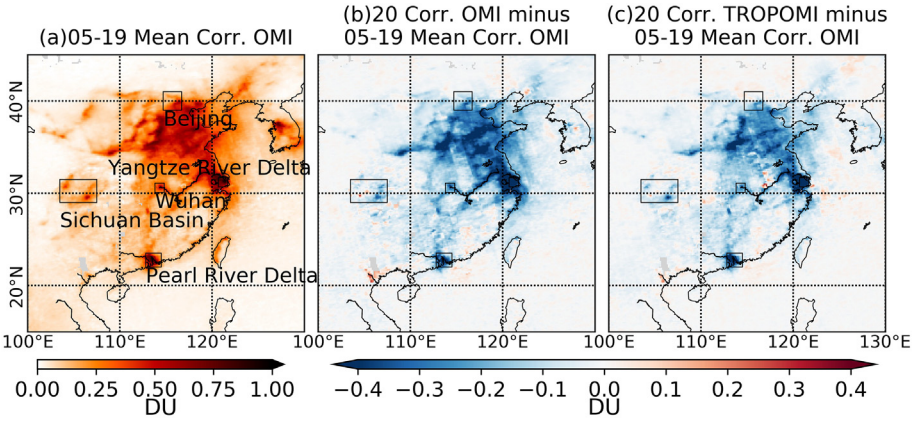

Fig. 3. (a) Climatological (2005–2019) tropospheric NO_2 vertical column density (VCDs) observed by OMI during lunar new year (LNY) holiday seasons in East China. (b) Tropospheric NO_2 reductions in 2020 observed by OMI relative to the 2005–2019 climatological mean from OMI. (c) Same as (b) but using TROPOMI 2020 data. All OMI/TROPOMI level 3 data are corrected using Eqs. (1)–(3).

(c) of Fig. 3, respectively. TropNO_2VCDs have decreased by 55%–72% over PRD, YRD and Wuhan metropolitans in 2020 LNY holiday season relative to mean TropNO_2VCDs of 2005–2019 LNY holiday seasons, while a smaller decrease of 33%–58% is observed in Beijing and Sichuan Basin. Both OMI and TROPOMI observations show that tropospheric NO_2 reductions occur mainly in the North China Plain and other metropolitan areas that are highly polluted with concentrated industrial and transportation sectors (Liu et al., 2016). Ground NO_2 concentrations have also been reported to decrease sharply during COVID-19 lockdowns globally (Collivignarelli et al., 2020; Lian et al., 2020; Tobías et al., 2020). This implies these tropospheric NO_2 reductions are strongly associated with the decline of industrial activities of COVID-19 lockdowns.

4.2. Characteristics of tropospheric NO_2 trends during LNY holiday seasons

TropNO_2VCDs had been increasing dramatically in China during the first decade of 21st century due to the rapid development of economy and industry (Richter et al., 2005; Zhang et al., 2018). Since 2010, the Chinese government has strengthened pollution control measures to reduce national emissions of nitrogen oxides by 10% by 2015 compared with 2010 NO_x emissions (de Foy et al., 2016; Hou et al., 2019; Zhang et al., 2018). TropNO_2VCDs in China started to decrease after reaching maximums around 2011–2012, depending on regions (Hou et al., 2019; Lin et al., 2019). These decreasing trends of TropNO_2VCDs in China were mainly caused by the clean air regulations, while the contribution of meteorological factors was negligible (<1%) (Lin et al., 2019). As result, the time series of TropNO_2VCDs over China indicate a "concave" shape with a peak around 2011–2012.

Time scales of weather patterns are approximately 1–2 weeks or less (Seinfeld and Pandis, 2016). The stochastic patterns imposed by weather systems will be averaged out in this study since we are averaging TropNO_2VCDs consistently over 40 days of LNY holiday seasons (European Centre for Medium-Range Weather Forecasts, 2020). Furthermore, to investigate the effect of meteorology on the reduction of TropNO_2VCDs, meteorological and climatological data of 2005–2020 LNY holidays have been investigated. These data include temperatures at 2 m above ground level (T2m) and 10 m (T10m), wind speed at 10 m above ground level (WS10m) from ERA5 (Hersbach et al., 2018) and MERRA-2 (Modern-Era Retrospective analysis for Research and Applications, Version 2) (Gelaro et al., 2017), wind speed at 100 m above ground level (WS100m) from ERA5 and wind speed at 50 m above ground level (WS50m) from MERRA-2. Meteorological conditions were normal during 2020 LNY holiday season, compared to climatological data of 2005–2019 LNY holiday seasons, as shown in Figs. S4–S9. For example, the median T2m is approximately 285 K over Wuhan in 2020 LNY holiday seasons as in Fig. S4, which is close to the median T2m of LNY holiday seasons in any year in 2005–2019. Consequently, meteorological and climatological conditions are assumed to have no significant influences on the reduction of tropospheric NO_2 over East China during 2020 LNY holiday season.

To capture the aforementioned "concave"-shape interannual variability, a quadratic regression model ($y = ax^2 + bx + c$) is utilized to fit the TropNO_2VCDs time series of 2005–2019 LNY holiday seasons, where x and y represent the year and TropNO_2VCDs averaged over LNY holiday season of that year. The expected TropNO_2VCDs during the 2020 LNY holiday season, without COVID-19 influence, can be predicted by linearly extrapolating the 2019 values with a slope of $2ax + b$, where $x = 2019$.

The predicted 2019–2020 changes of TropNO_2VCDs, calculated as the difference between 2019 values and predicted 2020 values, are plotted at the level 3 grid using OMI data in the panel (a) of Fig. 4. This

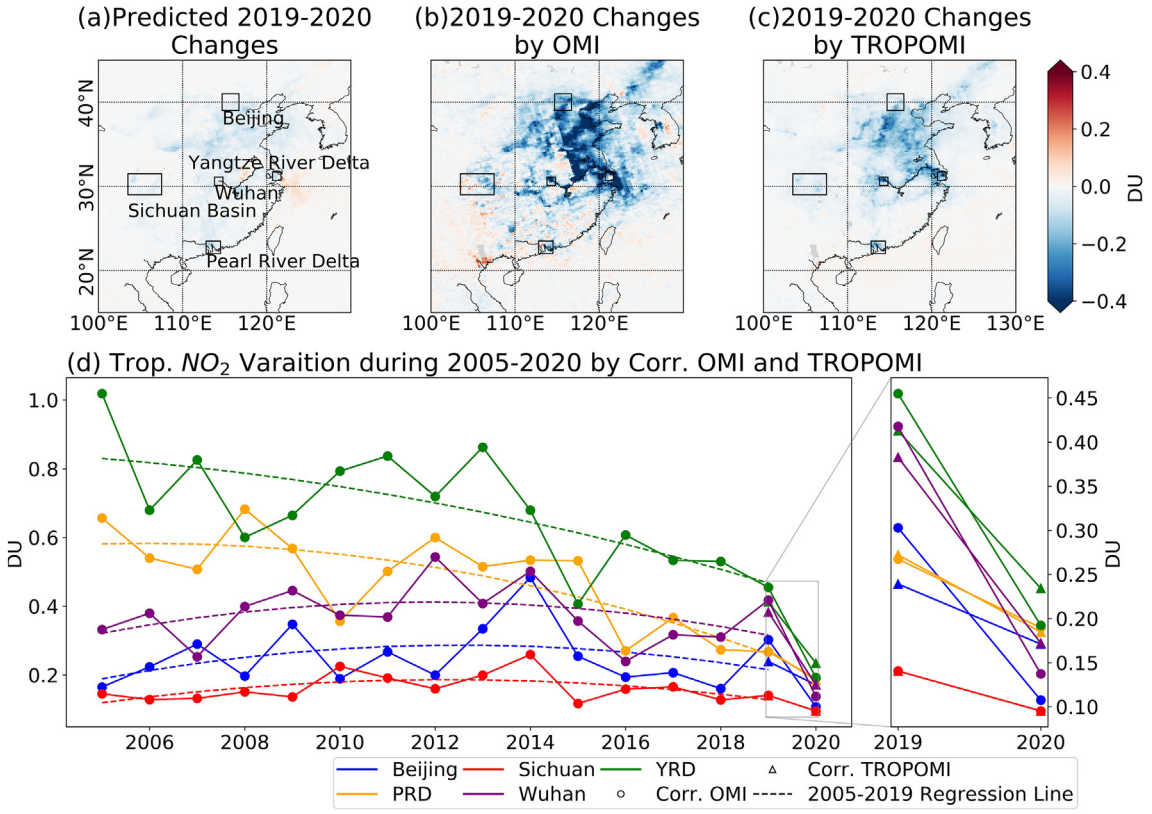

Fig. 4. Tropospheric NO_2 vertical column density (TropNO_2VCD) changes and variations over East China during lunar new year (LNY) holiday seasons by OMI and TROPOMI (with corrections applied). Panel (a) shows the predicted TropNO_2VCD changes during 2019–2020 LNY holidays, and panels (b) and (c) plot tropospheric NO_2 reductions over East China during 2019–2020 LNY, respectively, based on OMI and TROPOMI observations. Panel (d) shows temporal variations of TropNO_2VCDs during 2005–2020 LNY holiday seasons, with a zoom-in view for 2019–2020, in major metropolitan areas marked by different colors accordingly. The solid lines with solid dots and triangles represent TropNO_2VCDs in LNY holiday seasons observed by OMI and TROPOMI with correction applied, respectively. The dashed line with different colors represents tropospheric NO_2 regressions by the quadratic regression model in different metropolitan areas, accordingly.

change map indicates that TropNO$_2$VCDs have negative trends over East China, especially in the highly polluted North China Plain and other metropolitan areas, due to the clean air regulations of China. The real reductions of tropospheric NO$_2$ in 2019 and 2020 LNY holiday seasons, as observed by OMI and TROPOIMI, are ~1–9 times greater than the corresponding predicted changes (Fig. 4 (b)-(c)). Tropospheric VCDs declines by 22%–67% in the 2020 LNY holiday season relative to the 2019 LNY holiday season. These negative changes indicate that COVID-19 control measures and clean air regulations both contribute to reductions of tropospheric NO$_2$ in 2020 LNY holiday season over East China. The relative contributions by COVID-19 control measures and emission control varies over specific regions.

Fig. 4(d) shows temporal characteristics of LNY holiday season TropNO$_2$VCDs observed by OMI and TROPOMI with correction applied over major metropolitan areas. Table 1 lists predicted and observed 2019–2020 LNY holiday season changes by OMI and TROPOMI averaged over each region. Time series of TropNO$_2$VCDs indicate turning points after the conduction of clean air regulations of China over Beijing, Sichuan Basin and Wuhan metropolitan areas. TropNO$_2$VCDs are predicted to decrease by 0.022 DU, 0.017 DU and 0.027 DU in Beijing, Sichuan Basin and Wuhan metropolitan areas, respectively, between 2019 and 2020 LNY holiday seasons. In the PRD and YRD areas, TropNO$_2$VCDs show faster decreasing trends during LNY holiday seasons after the conduction of clean air regulations. TropNO$_2$VCDs are predicted to decrease by 0.049 DU and 0.041 DU in the PRD and YRD areas during 2019–2020 LNY holiday seasons, respectively.

Percentage contribution from the clean air regulations can be calculated as the predicted 2019–2020 tropospheric NO$_2$ changes divided by the observed 2019–2020 tropospheric NO$_2$ changes from OMI or TROPOMI. The percentage contribution from COVID-19 control measures is calculated as 100% minus percentage contribution from clean air regulations, since we assume the reduction of TropNO$_2$VCD is caused by COVID-19 control measures and clean air regulations. The ratios of emission control-caused and COVID-19 control measure-caused NO$_2$ reductions may reveal the impacts of COVID-19 lockdowns and control measures on tropospheric NO$_2$ variation in East China as shown in Table 1. In the Wuhan area, the first epicenter of the world, only ~10% (OMI) to 13% (TROPOMI) of the observed LNY tropospheric NO$_2$ reduction can be explained by the clean air regulations, while ~87%–90% of tropospheric NO$_2$ reduction is caused by the COVID-19 lockdowns because Wuhan had conducted the strictest lockdown and shelter-in-place regulations in the world (Tian et al., 2020). In the Beijing area, ~11%–32% and ~ 68%- 89% of the tropospheric NO$_2$ reduction is caused by the clean air regulations and COVID-19 control measures, as Beijing city has conducted considerably strict control measures (Beijing Municipal Health Commission, 2020). ~77%–84% and ~62% of the NO$_2$ reduction in YRD and Sichuan Basin is caused by the COVID-19 control measures, as cities of YRD (e.g., Shanghai City) and Sichuan Basin (e.g., Chengdu City and Chongqing City) had conducted similar control measures as Beijing city (Health Commission of Sichuan Province, 2020; Shanghai People's Government, 2020). In the YRD area, however, only ~37%–44% of the reduction is caused by the COVID-19 measures with the remaining ~56%–63% explained by the clean air regulations, due to less strict control measures (Health Commission of Guangdong Province, 2020). Overall, the ratio of NO$_2$ reduction caused by clean air regulations and COVID-19 control measures is associated with how strict the local COVID-19 control measures were conducted.

5. Discussions and conclusions

We studied the variation of TropNO$_2$VCDs in East China during the 2005–2020 LNY holiday seasons and the outbreak of COVID-19 by using OMI and TROPOMI tropospheric NO$_2$ observations. We have converted level 2 data of OMI and TROPOMI to 0.125° × 0.125° grid level 3 data by using the physical oversampling method (Sun et al., 2018) and applied corrections to OMI and TROPOMI NO$_2$ level 3 data to obtain a consistent dataset for this study. The corrections were obtained through the mean difference between OMI and TROPOMI tropospheric NO$_2$ in the 2019 and 2020 LNY holiday seasons.

TropNO$_2$VCDs had decreased sharply during 2020 LNY holiday season and the outbreak of COVID-19 in East China, especially in the North China Plain and other metropolitan areas. TropNO$_2$VCDs declines by ~33%–72% in 2020 LNY holiday seasons relative to 2005–2019 LNY holiday seasons and by 22%–67% relative to the 2019 LNY holiday season in East China. The meteorological contribution may be small because (1) meteorological conditions are normal in 2020 LNY holiday season, compared to climatological values of 2005–2019 LNY holiday seasons, and (2) our 40-day averaged TropNO$_2$VCDs have already averaged out stochastic patterns by weather systems. The impacts of NO$_x$ emission changes during LNY holiday seasons have been canceled out since the focus of this study is tropospheric NO$_2$ during LNY holiday seasons. Consequently, COVID-19 control measures and the clean air regulations of China are primary reasons for the reduction of TropNO$_2$VCDs over East China during the outbreak of COVID-19.

As the first epicenter, the Wuhan metropolitan area recorded ~54–64% tropospheric NO$_2$ reduction during 2020 LNY holiday season observed by TROPOMI and OMI, relative to the mean of 2005–2019 LNY holiday seasons. 2020 LNY holiday season TropNO$_2$VCDs in Beijing, YRD and PRD metropolitan areas are ~32%–72% less than the mean of 2005–2019 LNY holiday seasons, while the TropNO$_2$VCD in Sichuan Basin area during 2020 LNY holiday season is ~41% less than the mean value of 2005–2019.The reductions of tropospheric NO$_2$ in 2020 LNY holiday season relative to the 2019 LNY holiday season caused by the clean air regulations can be estimated by a quadratic regression model and 2005–2019 OMI TropNO$_2$VCDs. The clean air regulations have contributed to the reduction of TropNO$_2$VCDs by ~10%–63% over East China between 2019 and 2020 LNY holiday seasons. COVID-19 control measures are the primary factor for the reduction of tropospheric NO$_2$ and in most areas, while the clean air regulations are the primary factor in specific areas. The lockdowns of COVID-19 and clean air regulations has caused ~87%–90% and ~ 10%–13% of the tropospheric NO$_2$ reduction in the Wuhan area. COVID-19 control measures have caused ~68%–89%, ~77%–84% and ~62% of the tropospheric NO$_2$ reductions in Beijing, YRD and Sichuan Basin areas, respectively. The clean air regulations are the primary factor in the PRD area as the clean air regulations may explain ~56%–63% of the tropospheric NO$_2$ reduction. Overall, the primary and secondary factors for tropospheric NO$_2$ reduction are associated with how strict the COVID-19 control measures were conducted locally.

The COVID-19 control measures are the primary factor that causes a sharp reduction of tropospheric NO$_2$ in East China during the outbreak of COVID-19, while the contribution by the clean air regulations cannot be ignored. In specific areas, e.g. PRD area, the clean air regulation is the primary factor for the reduction of tropospheric NO$_2$. This study has focused on the variation of TropNO$_2$VCDs over specific periods of 2005–2020 when meteorological conditions were similar. However, NO$_x$ emissions and atmospheric chemistry conditions may be different. Further studies are needed to understand changes of NO$_x$ emissions and atmospheric chemistry as consequences of the COVID-19 pandemic.

CRediT authorship contribution statement

Guanyu Huang: Conceptualization, Methodology, Formal analysis, Investigation, Data curation, Writing - original draft, Visualization. **Kang Sun:** Methodology, Validation, Formal analysis, Writing - review & editing.

Declaration of competing interest

The authors declare that they have no known competing financial interests or personal relationships that could have appeared to influence the work reported in this paper.

Table 1
Predicted and observed (OMI and TROPOMI) changes of tropospheric NO_2 vertical column densities ($TropNO_2VCDs$) during 2019–2020 LNY holiday seasons over major metropolitan areas and corresponding percentage of tropospheric NO_2 reductions caused by the clean air regulations based on TROPOMI and OMI.

	Predicted 19–20 Changes (DU)	19–20 Changes by TROPOMI (DU)	19–20 Changes by OMI (DU)	Percentage of tropospheric NO_2 reduction caused by clean air regulations based on TROPOMI (%)	Percentage of tropospheric NO_2 reduction caused by clean air regulations based on OMI (%)
Beijing	−0.022	−0.068	−0.195	32	11
PRD	−0.049	−0.087	−0.078	56	63
Sichuan	−0.017	−0.045	−0.045	38	38
Wuhan	−0.027	−0.211	−0.28	13	10
YRD	−0.041	−0.179	−0.263	23	16

Acknowledgments

We acknowleage OMI and TROPOMI science teams for making OMI and TROPOMI level 2 data publically available. Kang Sun acknowledges support from NASA ACMAP and RRNES programs.

Funding

This research did not receive any specific grant from funding agencies in the public, commercial, or not-for-profit sectors.

Appendix A. Supplementary material

Supplementary material to this article can be found online at https://doi.org/10.1016/j.scitotenv.2020.141023.

References

Bauwens, M., Compernolle, S., Stavrakou, T., Müller, J.-F., Gent, J., Eskes, H., Levelt, P.F., A R., Veefkind, J.P., Vlietinck, J., Yu, H., Zehner, C., 2020. Impact of coronavirus outbreak on NO 2 pollution assessed using TROPOMI and OMI observations. Geophys. Res. Lett. e2020GL087978. doi:https://doi.org/10.1029/2020gl087978.

Beijing Municipal Health Commission, 2020. Beijing city COVID-19 prevention information. [WWW Document]. URL. http://wjw.beijing.gov.cn/wjwh/ztzl/xxgzbd/gzbdzcfg/index.html (Accessed 3 June 2020).

Bucsela, E.J., Krotkov, N.A., Celarier, E.A., Lamsal, L.N., Swartz, W.H., Bhartia, P.K., Boersma, K.F., Veefkind, J.P., Gleason, J.F., Pickering, K.E., 2013. A new stratospheric and tropospheric NO_2 retrieval algorithm for nadir-viewing satellite instruments: applications to OMI. Atmos. Meas. Tech 6, 2607–2626. https://doi.org/10.5194/amt-6-2607-2013.

Cheng, S., Ma, J., Cheng, W., Yan, P., Zhou, H., Zhou, L., Yang, P., 2019. Tropospheric NO 2 vertical column densities retrieved from ground-based MAX-DOAS measurements at Shangdianzi regional atmospheric background station in China. J. Environ. Sci. (China) 80, 186–196. https://doi.org/10.1016/j.jes.2018.12.012.

Collivignarelli, M.C., Abbà, A., Bertanza, G., Pedrazzani, R., Ricciardi, P., Carnevale Miino, M., 2020. Lockdown for CoViD-2019 in Milan: what are the effects on air quality? Sci. Total Environ. 732, 139280. https://doi.org/10.1016/j.scitotenv.2020.139280.

Duncan, B.N., Lamsal, L.N., Thompson, A.M., Yoshida, Y., Lu, Z., Streets, D.G., Hurwitz, M.M., Pickering, K.E., 2016. A space-based, high-resolution view of notable changes in urban NOx pollution around the world (2005–2014). J. Geophys. Res. 121, 976–996. https://doi.org/10.1002/2015JD024121.

Earth Observatory NASA, 2020. Airborne Nitrogen Dioxide Plummets Over China. WWW Document. Earth Obs. NASA URL. https://earthobservatory.nasa.gov/images/146362/airborne-nitrogen-dioxide-plummets-over-china (Accessed 28 April 2020).

Eskes, H.J., Eichmann, K.-U., 2019. S5P Mission Performance Centre Nitrogen Dioxide [L2__NO2___] Readme. https://doi.org/10.5270/S5P-s4ljg54.

European Centre for Medium-Range Weather Forecasts, 2020. Flawed estimates of the effects of lockdown measures on air quality derived from satellite observations| Copernicus. [WWW Document]. URL. https://atmosphere.copernicus.eu/flawed-estimates-effects-lockdown-measures-air-quality-derived-satellite-observations (Accessed 1 June 2020).

European Space Agency, 2018. TROPOMI Level 2 Nitrogen Dioxide Total Column Products, Version 01. https://doi.org/10.5270/S5P-s4ljg54.

Feng, J., Yu, H., Su, X., Liu, S., Li, Y., Pan, Y., Sun, J.H., 2016. Chemical composition and source apportionment of PM2.5 during Chinese spring festival at Xinxiang, a heavily polluted city in North China: fireworks and health risks. Atmos. Res. 182, 176–188. https://doi.org/10.1016/j.atmosres.2016.07.028.

de Foy, B., Lu, Z., Streets, D.G., 2016. Satellite NO2 retrievals suggest China has exceeded its NOx reduction goals from the twelfth five-year plan. Sci. Rep. 6, 35912. doi:https://doi.org/10.1038/srep35912https://www.nature.com/articles/srep35912#supplementary-information.

Gelaro, R., McCarty, W., Suárez, M.J., Todling, R., Molod, A., Takacs, L., Randles, C.A., Darmenov, A., Bosilovich, M.G., Reichle, R., Wargan, K., Coy, L., Cullather, R., Draper, C., Akella, S., Buchard, V., Conaty, A., Silva, A.M. da, Gu, W., Kim, G.-K., Koster, R., Lucchesi, R., Merkova, D., Nielsen, J.E., Partyka, G., Pawson, S., Putman, W., Rienecker, M., Schubert, S.D., Sienkiewicz, M., Zhao, B., 2017. The modern-era retrospective analysis for research and applications, version 2 (MERRA-2). J. Clim. 30, 5419–5454. https://doi.org/10.1175/jcli-d-16-0758.1.

Griffin, D., Zhao, X., McLinden, C.A., Boersma, F., Bourassa, A., Dammers, E., Degenstein, D., Eskes, H., Fehr, L., Fioletov, V., Hayden, K., Kharol, S.K., Li, S.-M., Makar, P., Martin, R.V., Mihele, C., Mittermeier, R.L., Krotkov, N., Sneep, M., Lamsal, L.N., Linden, M. ter, Geffen, J. van, Veefkind, P., Wolde, M., 2019. High-resolution mapping of nitrogen dioxide with TROPOMI: first results and validation over the Canadian oil sands. Geophys. Res. Lett. 46, 1049–1060. https://doi.org/10.1029/2018GL081095.

Health Commission of Guangdong Province, 2020. COVID-19 news of Guangdong province. [WWW Document]. URL. http://wsjkw.gd.gov.cn/xxgzbdfk/ (Accessed 3 June 2020).

Health Commission of Sichuan Province, 2020. Sichuan COVID-19 prevention news. [WWW Document]. URL. http://wsjkw.sc.gov.cn/scwsjkw/gzbd/fyzt.shtml (Accessed 3 June 2020).

Hersbach, H., De Rosnay, P., Bell, B., Schepers, D., Simmons, A., Soci, C., Abdalla, S., Balmaseda, A., Balsamo, G., Bechtold, P., Berrisford, P., Bidlot, J., De Boisséson, E., Bonavita, M., Browne, P., Buizza, R., Dahlgren, P., Dee, D., Dragani, R., Diamantakis, M., Flemming, J., Forbes, R., Geer, A., Haiden, T., Hólm, E., Haimberger, L., Hogan, R., Horányi, A., Janisková, M., Laloyaux, P., Lopez, P., Muñoz-Sabater, J., Peubey, C., Radu, R., Richardson, D., Thépaut, J.-N., Vitart, F., Yang, X., Zsótér, E., Zuo, H., 2018. Operational global reanalysis: progress, future directions and synergies with NWP including updates on the ERA5 production status. ERA Report Series https://doi.org/10.21957/tkic6g3wm.

Hou, Y., Wang, L., Zhou, Y., Wang, S., Liu, W., Zhu, J., 2019. Analysis of the tropospheric column nitrogen dioxide over China based on satellite observations during 2008–2017. Atmos. Pollut. Res. https://doi.org/10.1016/j.apr.2018.11.003.

Huang, K., Zhuang, G., Lin, Y., Wang, Q., Fu, J.S., Zhang, R., Li, J., Deng, C., Fu, Q., 2012. Impact of anthropogenic emission on air quality over a megacity – revealed from an intensive atmospheric campaign during the Chinese spring festival. Atmos. Chem. Phys. 12, 11631–11645. https://doi.org/10.5194/acp-12-11631-2012.

Ji, D., Cui, Y., Li, L., He, J., Wang, L., Zhang, H., Wang, W., Zhou, L., Maenhaut, W., Wen, T., Wang, Y., 2018. Characterization and source identification of fine particulate matter in urban Beijing during the 2015 spring festival. Sci. Total Environ. 628–629, 430–440. https://doi.org/10.1016/j.scitotenv.2018.01.304.

Kroon, M., Dobber, M.R., Dirksen, R., Veefkind, J.P., van den Oord, G.H.J., Levelt, P.F., 2008. Ozone monitoring instrument geolocation verification. J. Geophys. Res. 113. https://doi.org/10.1029/2007JD008821.

Krotkov, N.A., Lamsal, L.N., Celarier, E.A., Swartz, W.H., Marchenko, S.V., Bucsela, E.J., Chan, K.L., Wenig, M., Zara, M., 2017. The version 3 OMI NO $_2$ standard product. Atmos. Meas. Tech 10, 3133–3149. https://doi.org/10.5194/amt-10-3133-2017.

Krotkov, N.A., Lamsal, L.N., Marchenko, S. V., Celarier, E.A., J. Bucsela, E., Swartz, W.H., Joiner, J., Team, the O. core, 2019. OMI/Aura Nitrogen Dioxide (NO2) Total and Tropospheric Column 1-orbit L2 Swath 13×24 km V003. doi:https://doi.org/10.5067/Aura/OMI/DATA2017.

Levelt, P.F., Hilsenrath, E., Leppelmeier, G.W., van den Oord, G.H.J., Bhartia, P.K., Tamminen, J., de Haan, J.F., Veefkind, J.P., 2006. Science objectives of the ozone monitoring instrument. IEEE Trans. Geosci. Remote Sens. 44, 1199–1208.

Li, J., Ye, Q., Deng, X., Liu, Yaolin, Liu, Yanfang, 2016. Spatial-temporal analysis on spring festival travel rush in China based on multisource big data. Sustainability 8, 1184. https://doi.org/10.3390/su8111184.

Li, Q., Guan, X., Wu, P., Wang, X., Zhou, L., Tong, Y., Ren, R., Leung, K.S.M., Lau, E.H.Y., Wong, J.Y., Xing, X., Xiang, N., Wu, Y., Li, C., Chen, Q., Li, D., Liu, T., Zhao, J., Liu, M., Tu, W., Chen, C., Jin, L., Yang, R., Wang, Q., Zhou, S., Wang, R., Liu, H., Luo, Y., Liu, Y., Shao, G., Li, H., Tao, Z., Yang, Y., Deng, Z., Liu, B., Ma, Z., Zhang, Y., Shi, G., Lam, T.T.Y., Wu, J.T., Gao, G.F., Cowling, B.J., Yang, B., Leung, G.M., Feng, Z., 2020. Early transmission dynamics in Wuhan, China, of novel coronavirus–infected pneumonia. N. Engl. J. Med. https://doi.org/10.1056/nejmoa2001316.

Lian, X., Huang, J., Huang, R., Liu, C., Wang, L., Zhang, T., 2020. Impact of city lockdown on the air quality of COVID-19-hit of Wuhan city. Sci. Total Environ. 742, 140556. https://doi.org/10.1016/j.scitotenv.2020.140556.

Lin, J.-T., 2012. Satellite constraint for emissions of nitrogen oxides from anthropogenic, lightning and soil sources over East China on a high-resolution grid. Atmos. Chem. Phys. 12, 2881–2898. https://doi.org/10.5194/acp-12-2881-2012.

Lin, N., Wang, Y., Zhang, Y., Yang, K., 2019. A large decline of tropospheric NO2 in China observed from space by SNPP OMPS. Sci. Total Environ. 675, 337–342. https://doi.org/10.1016/J.SCITOTENV.2019.04.090.

Liu, F., Zhang, Q., van der A, R.J., Zheng, B., Tong, D., Yan, L., Zheng, Y., He, K., 2016. Recent reduction in NO $_x$ emissions over China: synthesis of satellite observations and emission inventories. Environ. Res. Lett. 11, 114002. doi:https://doi.org/10.1088/1748-9326/11/11/114002.

Liu, F., Page, A., Strode, S.A., Yoshida, Y., Choi, S., Zheng, B., Lamsal, L.N., Li, C., Krotkov, N.A., Eskes, H., A. R. van der, Veefkind, P., Levelt, P.F., Hauser, O.P., Joiner, J., 2020. Abrupt decline in tropospheric nitrogen dioxide over China after the outbreak of COVID-19. Sci. Adv. eabc2992. doi:https://doi.org/10.1126/sciadv.abc2992.

Richter, A., Burrows, J.P., Nüß, H., Granier, C., Niemeier, U., 2005. Increase in tropospheric nitrogen dioxide over China observed from space. Nature 437, 129–132. https://doi.org/10.1038/nature04092.

Seinfeld, J.H., Pandis, S.N., 2016. Atmospheric Chemistry and Physics: From Air Pollution to Climate Change. 3rd edition. Wiley. John Wiley & Sons.

Shah, V., Jacob, D.J., Li, K., Silvern, R.F., Zhai, S., Liu, M., Lin, J., Zhang, Q., 2020. Effect of changing NO_{<i>x</i>} lifetime on the seasonality and long-term trends of satellite-observed tropospheric NO₂ columns over China. Atmos. Chem. Phys. 20, 1483–1495. https://doi.org/10.5194/acp-20-1483-2020.

Shanghai People"s Government, 2020. Shanghai COVID-19 prevention news. [WWW Document]. URL. http://www.shanghai.gov.cn/nw2/nw2314/nw32419/nw48516/index.html (Accessed 3 June 2020).

Sun, K., Zhu, L., Cady-Pereira, K., Chan Miller, C., Chance, K., Clarisse, L., Coheur, P.-F.F., González Abad, G., Huang, G., Liu, X., Van Damme, M., Yang, K., Zondlo, M., 2018. A physics-based approach to oversample multi-satellite, multispecies observations to a common grid. Atmos. Meas. Tech 11, 6679–6701. https://doi.org/10.5194/amt-11-6679-2018.

Tan, P.H., Chou, C., Liang, J.Y., Chou, C.C.K., Shiu, C.J., 2009. Air pollution "holiday effect" resulting from the Chinese new year. Atmos. Environ. 43, 2114–2124. https://doi.org/10.1016/j.atmosenv.2009.01.037.

Tian, H., Liu, Y., Li, Y., Wu, C.-H., Chen, B., Kraemer, M.U.G., Li, B., Cai, J., Xu, B., Yang, Q., Wang, B., Yang, P., Cui, Y., Song, Y., Zheng, P., Wang, Q., Bjornstad, O.N., Yang, R., Grenfell, B.T., Pybus, O.G., Dye, C., 2020. An investigation of transmission control measures during the first 50 days of the COVID-19 epidemic in China. Science (80-.), eabb6105 https://doi.org/10.1126/science.abb6105.

Tobías, A., Carnerero, C., Reche, C., Massagué, J., Via, M., Minguillón, M.C., Alastuey, A., Querol, X., 2020. Changes in air quality during the lockdown in Barcelona (Spain) one month into the SARS-CoV-2 epidemic. Sci. Total Environ. 726, 138540. https://doi.org/10.1016/j.scitotenv.2020.138540.

Veefkind, J.P., Aben, I., McMullan, K., Förster, H., de Vries, J., Otter, G., Claas, J., Eskes, H.J., de Haan, J.F., Kleipool, Q., van Weele, M., Hasekamp, O., Hoogeveen, R., Landgraf, J., Snel, R., Tol, P., Ingmann, P., Voors, R., Kruizinga, B., Vink, R., Visser, H., Levelt, P.F., 2012. TROPOMI on the ESA Sentinel-5 precursor: A GMES mission for global observations of the atmospheric composition for climate, air quality and ozone layer applications. Remote Sens. Environ. 120, 70–83. https://doi.org/10.1016/j.rse.2011.09.027.

World Health Organization, 2020. Novel Coronavirus (2019-nCoV) Situationa Report-1, 21 January 2020.

Yao, L., Wang, D., Fu, Q., Qiao, L., Wang, H., Li, L., Sun, W., Li, Q., Wang, L., Yang, X., Zhao, Z., Kan, H., Xian, A., Wang, G., Xiao, H., Chen, J., 2019. The effects of firework regulation on air quality and public health during the Chinese Spring Festival from 2013 to 2017 in a Chinese megacity. Environ. Int. 126, 96–106. https://doi.org/10.1016/j.envint.2019.01.037.

Zhang, X., Zhang, W., Lu, X., Liu, X., Chen, D., Liu, L., Huang, X., 2018. Long-term trends in NO2 columns related to economic developments and air quality policies from 1997 to 2016 in China. Sci. Total Environ. 639, 146–155. https://doi.org/10.1016/j.scitotenv.2018.04.435.

Zhang, J., Huang, X., Chen, Y., Luo, B., Luo, J., Zhang, W., Rao, Z., Yang, F., 2019. Characterization of lead-containing atmospheric particles in a typical basin city of China: seasonal variations, potential source areas, and responses to fireworks. Sci. Total Environ. 661, 354–363. https://doi.org/10.1016/j.scitotenv.2019.01.079.

Zhu, L., Jacob, D.J., Keutsch, F.N., Mickley, L.J., Scheffe, R., Strum, M., González Abad, G., Chance, K., Yang, K., Rappenglück, B., Millet, D.B., Baasandorj, M., Jaeglé, L., Shah, V., 2017. Formaldehyde (HCHO) as a hazardous air pollutant: mapping surface air concentrations from satellite and inferring cancer risks in the United States. Environ. Sci. Technol. 51, 5650–5657. https://doi.org/10.1021/acs.est.7b01356.